Chemical Physics Letters: X 3 (2019) 100029

Contents lists available at ScienceDirect

Chemical Physics Letters: X

journal homepage: www.journals.elsevier.com/chemical-physics-letters-x

Quantification of nitric acid using photolysis induced fluorescence for use in chemical kinetic studies

Frank A.F. Winiberg[a,b], Carl J. Percival[a], Stanley P. Sander[a,*]

[a] NASA Jet Propulsion Laboratory, California Institute of Technology, Pasadena, CA 91109, USA
[b] California Institute of Technology, Pasadena, CA 91109, USA

HIGHLIGHTS

- Single and two photon photodissociation of gas phase nitric acid at 248 and 193 nm.
- Three emissions from excited products have been identified spectroscopically.
- Nitric acid can be quantified based on the intensity of these emissions.
- Established a unique detection method for the future study of nitric acid kinetics.

ABSTRACT

Previous laboratory investigations have predominantly relied on UV absorption measurement of [HNO_3]. Whilst direct, this measurement is difficult at temperatures < 298 K, where heterogeneous loss to cold surfaces is significant. Single and two photon photodissociation of HNO_3 was studied in N_2 and He at 193 and 248 nm, and a unique HNO_3 detection method was established using two photons at 248 nm, with good reproducibility and limit of detection (~1.25×10^{14} cm^{-3}). Emissions from excited products have been identified spectroscopically, over a range of pressures and laser energies to support the HNO_3 quantification method.

1. Introduction

Nitric acid (HNO_3) is an important atmospheric species that plays a key role in determining the production and destruction of O_3 by controlling the balance of NO_x (=NO + NO_2) and HO_x (=OH + HO_2) radicals in the upper troposphere/lower stratosphere. Produced primarily through the reaction of OH + NO_2, HNO_3 acts as a reservoir for higher oxides of nitrogen (NO_y) removing NO_2 and forming nitrate radicals via reaction with OH, OH + $HNO_3 \rightarrow H_2O$ + NO_3. The reaction of HNO_3 with OH has been shown to be very important for governing the balance of NO_x/NO_y.

In kinetics experiments, as well as in the field, characterization of accurate HNO_3 concentrations is important. Previous laboratory investigations into the temperature and pressure dependent rate coefficient for the OH + HNO_3 reaction have predominantly relied on the UV absorption measurement of [HNO_3], e.g. [17,4,15,3]. Whilst direct, the absorption measurement is difficult at temperatures < 298 K where heterogeneous loss of the HNO_3 to the cold reactor surfaces can become significant. Uptake of HNO_3 can lead to concentration gradients across an *in-situ* measurement axis, and overall loss of HNO_3 for an *ex-situ* absorption axis. Therefore, both methods could underestimate [HNO_3] and ultimately overestimate the OH + HNO_3 rate coefficient. Utilizing a detection method that probes the HNO_3 in the reaction zone would therefore be beneficial for the continued study of this important reaction.

Previously, Photolysis Induced Fluorescence (PIF) has been used as an indirect method to measure HNO_3 [8], whereby photolytic generation of exited state products results in radiative decay to their ground state. The photodissociation chemistry of nitric acid is complex and has received considerable attention in the literature, both experimental and theoretical. Depending on the wavelength of the excitation, several dissociation pathways are available:

$$HNO_3 + h\nu \rightarrow OH(X^2\Pi) + NO_2(X^2A_1)\Delta H^o = 200 \text{ kJ mol}^{-1} \text{ (598 nm)} \quad (1)$$

$$\rightarrow OH(X^2\Pi) + NO_2(1^2B_2)\Delta H^o = 315 \text{ kJ mol}^{-1} \text{ (380 nm)} \quad (2)$$

$$\rightarrow O(^1D) + HONO(X^1A')\Delta H^o = 490 \text{ kJ mol}^{-1} \text{ (244 nm)} \quad (3)$$

$$\rightarrow O(^3P + HONO(a^3A'')\Delta H^o = 550 \text{ kJ mol}^{-1} \text{ (218 nm)} \quad (4)$$

* Corresponding author.
E-mail address: Stanley.Sander@jpl.nasa.gov (S.P. Sander).

https://doi.org/10.1016/j.cpletx.2019.100029
Received 27 November 2018; Received in revised form 19 March 2019; Accepted 20 March 2019
Available online 22 April 2019

$$\rightarrow O(^3P) + HONO(X^1A)\Delta H^o = 300\ kJ\ mol^{-1}\ (399\ nm) \quad (3)$$

Low energy photolysis (> 280 nm) yields predominantly OH + NO_2, and high energy photolysis (< 260 nm) produces a combination of O + HONO and OH + NO_2 products [16,12,10,7]. Theoretical photodissociation pathways for the four lowest electronic singlet states (S_0, S_1, S_2 and S_3) support experimental quantum yield observations and have provided a useful insight into the energetically favored branching pathways for this complicated system [1,19].

Kenner et al. [8] investigated the two-photon pumping of HNO_3 using 193 nm light from two excimer lasers. Intense emissions around 308 nm were observed, and a new method of HNO_3 field measurements was proposed. More recently, used the two photon photolysis of HNO_3 at 193 nm to accurately measure [HNO_3] in a series of OH + HNO_3 kinetics experiments. conducted a three laser experiment: 248 nm to initiate the OH chemistry, 193 nm to probe [HNO_3] (with a focused beam) and 282 nm to probe the OH radicals. Based on the initial experiments of Kenner et al. [8], we have investigated the single and two-photon pumping of HNO_3 at 248 nm for the quantification of HNO_3. By utilizing a single 248 nm excimer laser, we have reduced the complexity of the apparatus used for the study of chemical kinetics of OH + HNO_3 [18]. In this paper, we show the empirical calibration procedure for the fluorescence intensity observed from the two photon photolysis of HNO_3, measuring the [HNO_3] using VUV absorption. To aid in the analysis and characterization of the system, we have also conducted some HNO_3 photolysis experiments at 193 nm.

2. Experimental

The apparatus used in this study has been described previously by Mollner et al. [9] and so only the modifications to the system will be discussed here (diagram: Figure S1). The pulsed laser photolysis apparatus is normally used in combination with Laser Induced Fluorescence (LIF) to track the kinetic profile of OH radicals in a pseudo first order environment. Here, the LIF laser system was not used.

Mass flow controllers (MKS) were used to control the flow of gas into the cell, and the desired bath gas pressure (50–750 Torr) was maintained using an automated valve and pressure controller. Reaction cell pressures were monitored using two pressure gauges (MKS, 10 and 1000 Torr) on the gas-outflow. Reactants were mixed with bath gas (N_2 or He) in a 5-port glass manifold ~50 cm before entering the cell. Flow rates were chosen so that the residence time in the photolysis region was ~50 ms, ensuring a fresh sample of gas between each laser shot from the photolysis laser (20 Hz Pulse Repetition Frequency).

Gas phase HNO_3 was introduced into the cell by flowing 3–100 sccm of N_2/He through a bubbler containing a 1:3 mixture of $HONO_2$ (70% in H_2O) and H_2SO_4 (conc.). The bubbler was maintained at ~200 Torr total pressure across all experiments carried out over the pressure range 50–200 Torr, however was held at the same pressure as the reactor (350–750 Torr) for pressures > 200 Torr.

2.1. Fluorescence detection

To examine the two photon photolysis of HNO_3, the excimer laser output was focused into the center of the reaction cell (UV-fused silica plano-convex, f = 1000 mm). Emissions were collected onto 3 different detectors: two photomultiplier tubes (PMT, PC25, Sens-Tech) and one Intensified CCD (ICCD, PI-MAX Gen II). The first PMT doubles as the LIF PMT when the cell is being used in its primary configuration – for the study of OH radicals – perpendicular to the excimer beam and with a 310 ± 5 nm narrow bandpass filter positioned in-between two light collection optics and a series of baffles to exclude scattered light. This PMT was deployed to collect the UV emission from the excited photodissociation products of the two photon HNO_3 photolysis. The second PMT and the ICCD were positioned in the same plane as the excimer beam, at a 45° angle. Light collection optics were mounted internally by fixing lenses (f = 50 mm) to the end of 1″ O.D. glass tubing using a vacuum compatible epoxy adhesive (Torr-Seal). The opposite end of the glass side arms were sealed using a 5 mm thick 1″ UV fused silica window, and were evacuated through a glass valve, to avoid unwanted absorption or scattering of emitted light from ambient air in the optical path.

Light collimated from the center of the cell was directed towards a second PMT or imaged onto an ICCD. After passing through the glass side arm, a set of baffles and a second lens (1″, f = 75 mm), was used to refocus the light onto the photocathode of the second PMT. The baffles included a 650 ± 50 nm bandpass filter (Thorlabs), aimed at collecting longer wavelength emissions from the single photon photolysis of HNO_3. Finally, light was directed into an Acton 300i spectrograph using a lens (1″, f = 100 mm, Thorlabs) and imaged onto the ICCD. Images from the ICCD were integrated over 100 ns per laser shot (from t_0) and normalized to the instrument wavelength response curve. Spectra recorded in the UV region used an entrance slit width of 50 µm combined with a 3600 g/mm grating, giving a spectral resolution of 0.08 nm. Spectra recorded in the visible region used an entrance slit width of 100 µm combined with a 600 g/mm grating, giving a spectral resolution of ~1 nm.

2.2. HNO_3 detection

HNO_3 was detected using VUV absorption at 185 nm, *ex-situ*. The absorption measurement cell had a diameter of 2.5 cm, 50 cm length, sealed with Suprasil windows and was positioned after the fluorescence cell (see Figure S1).

The 185 nm output of an Hg-Ar penray lamp (LOT-Oriel) was used in combination with three narrow-bandpass filters (LOT-Oriel, (185 ± 10) nm (FWHM)) to exclude the longer wavelength emissions from the Hg lamp. Light was detected using a photomultiplier tube (PMT, LOT-Oriel).

The absorption cross-section for HNO_3 at 185 nm, $\sigma_{185\ nm}$, has been determined several times in the literature [2,17,4]. In a recent study, used a meticulous approach to account for a variety of impurities (NO_2, NO_3, N_2O_5 and H_2O), measuring at two wavelengths simultaneously, and ultimately found their value to agree within experimental error of the previous studies. We therefore use the $\sigma_{185\ nm}$ determined in the study by ($= (1.6 \pm 0.1) \times 10^{-17}$ cm^2).

2.3. Excimer conditions

Nitric acid was photolyzed using the 193 and 248 nm output of an excimer laser (LPX 120i, Lambda Physik) filled with ArF and KrF gas mixtures respectively. The laser was operated in two modes: unfocussed (single photon) and focused (two photon). The excimer beam was focused into the center of the reactor for the two photon mode, using a f = 1000 mm UV fused silica lens in a flip-mount.

3. Results and discussion

3.1. Single photon photolysis

3.1.1. 248 nm excitation

Fig. 1 shows the measured emission spectrum between 350 and 800 nm measured at 50 Torr N_2, [HNO_3] ~ 2×10^{15} cm^{-3}, averaged over 10,000 laser shots and using an unfocused excimer beam (180 mJ) at 248 nm. Possible 2nd and 3rd order grating diffraction emissions were removed using a longpass filter (Schott GG-400) placed before the spectrograph. This filter blocks any emission below 400 nm. Using a PMT/ filter combination (650 ± 50 nm), the intensity of the emission was observed to be linear as a function of laser power, indicating a single photon photolysis process (Fig. 2a). The emission intensity was also observed to increase linearly with respect to [HNO_3] (see supplement Figure S2). Above 350 Torr it was difficult to discriminate

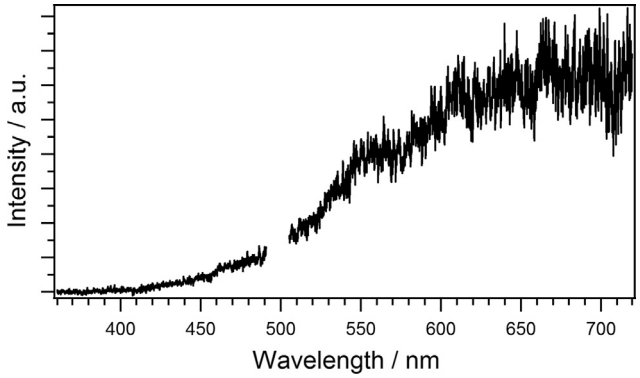

Fig. 1. Emission spectrum observed from the single photon photolysis of HNO_3 at 248 nm measured at 50 Torr N_2, $[HNO_3] \sim 2 \times 10^{15}$ cm^{-3} and an unfocussed excimer beam (180 mJ). Fluorescence spectrum is likely emission from electronically excited $NO_2(^1B_2)$ produced on the S_2 surface of HNO_3. Scatter from second order grating diffraction of the 248 nm excimer pulse was removed ~496 nm.

between NO_2 emission and background scattered light as a result of poor signal to noise. The HNO_3 fluorescence has a fast decay (< 100 ns), faster than the minimum time resolution of our collection apparatus, thus it was not possible to measure the decay lifetime as a function of pressure or $[HNO_3]$.

The broad, featureless emission at wavelengths > 400 nm (Fig. 1) is likely emission from $NO_2(^1B_2)$, formed on the S_2 surface of the HNO_3. Sinha et al. [14] reported chemiluminescence when exciting HNO_3 with a single photon at 260 nm, which they assigned to an excited state of NO_2. Emission from an excited state of NO_2 is supported by the fact that the emission occurs above the dissociation energy of NO_2 (398 nm), and the appearance is consistent with Derro et al. [5], who reported an emission from an excited NO_2 photofragment in the photodissociation of nitrites. A recent computational study by Xiao et al. [19] showed that, at 248 nm, the photodissociation of HNO_3 leads almost exclusively to the OH(X) + $NO_2(^1B_2)$ products on the S_2 surface – in line with the observations here.

For the purpose of HNO_3 quantification, however, the value of the single photon PIF method at 248 nm is limited and was not used in the further chemical kinetic study of OH + HNO_3 [18]. The accurate measurement of $[HNO_3]$ was only possible at pressures < 350 Torr, whereas total pressures up to 750 Torr are required for the OH + HNO_3 kinetic system. Additionally, the limit of detection (LOD: 1.7–7.0 × 10^{14} cm^{-3} from 50 to 350 Torr) was above the desired minimum concentration required ($[HNO_3]_{min} \sim 1 \times 10^{14}$ cm^{-3}). Therefore, for HNO_3 quantification we used two-photon PIF as described below.

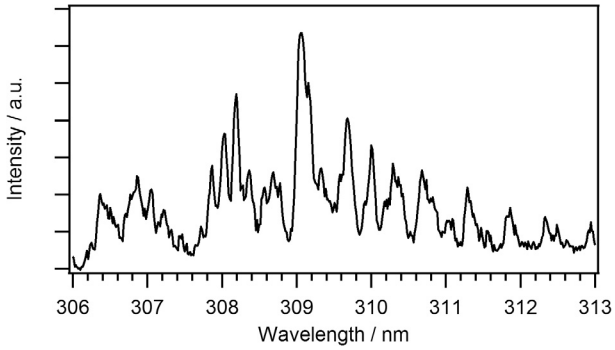

Fig. 3. Spectrum of the OH (A → X, $v' = 0$, $v'' = 0$) emission from the two photon photolysis of HNO_3 at 248 nm; 30,000 laser shots. Rotational temperature ~800 K.

3.2. Two photon photolysis

3.2.1. 248 nm excitation

The emission spectrum between 306 and 313 nm for the 248 nm, two photon initiated photolysis of HNO_3 is shown in Fig. 3. The spectrum was collected at 50 Torr N_2, $[HNO_3] \sim 2 \times 10^{15}$ cm^{-3} and with a focused excimer beam (120 mJ). The emission required extensive averaging (30000 laser shots per spectral window) to achieve the signal-to-noise required for qualitative analysis of the spectrum, hence only one region of interest was targeted.

The spectral features were identified OH(A → X, $v' = 0$, $v'' = 0$) at ~309 nm with an approximate rotational temperature of 800 K. Using a PMT connected to the spectrograph, intensities measured at both 226 and 309 nm were observed to have a squared dependence with laser power (Fig. 2b), suggesting a two-photon photolysis process that produces both excited OH and NO species. Kenner et al. [8] also observed

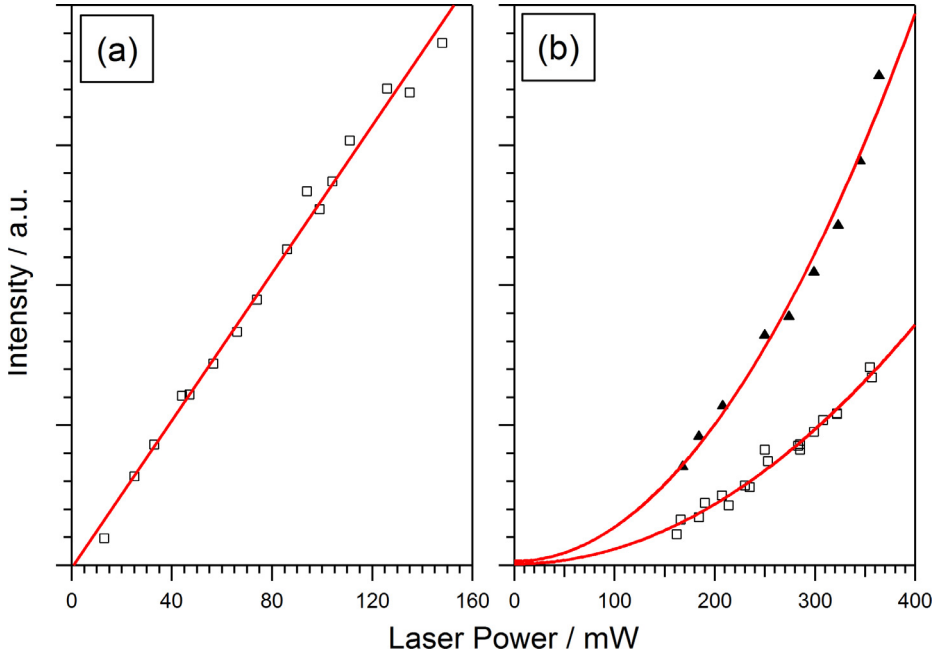

Fig. 2. The integrated signal intensity at (a) 650 nm and (b) 308 nm as a function of excimer laser power; $\lambda_{EX} = 248$ nm, 2000 shots per point, $[HNO_3] = 1 \times 10^{15}$ cm^{-3}. (a) Unfocussed excimer beam (single photon), data have been fit with a linear function; (b) Focused excimer beam (two photon); fluorescence sampled at (□) 308 nm and (▲) 226 nm to target the OH ($A \rightarrow X$, $v' = 0$, $v'' = 0$) and NO ($A \rightarrow X$, $v' = 0$, $v'' = 0$) fluorescence respectively; data have been fit with a quadratic function, $y = y_0 + Ax^2$.

an emission at ~308 nm from the two photon pumping of HNO_3 at 248 nm, which they believed to be OH(A → X).

It is possible that the observed emissions were due to the photolysis of an impurity in the HNO_3 sample used, e.g. NO_2, however NO(A → X) or OH(A → X) fluorescence was not observed from the photolysis of pure NO_2 samples ($[NO_2] = 0.2–1.5 \times 10^{15}$ cm^{-3}). Additionally, the absence of NO_2 in the reaction cell was confirmed using a 50 cm ex-situ absorption cell coupled to a quartz halogen lamp and spectrograph with CCD (Acton 300i and Princeton Instruments PIXIS 100). Based on the $[HNO_3]$ produced during this test (~1×10^{15} cm^{-3}) and the NO_2 limit of detection of the apparatus (~5×10^{12} cm^{-3}), the NO_2 impurity was established to be < 1%, below the $[NO_2]$ used in the control experiments.

The observation of OH(A → X) and NO(A → X) fluorescence is somewhat unexpected in this system when pumping HNO_3 at 248 nm. Using light at 193 nm, Kenner et al. [8] and hypothesized a channel to OH(A → X) through a bifurcated HNO_3 S_3 surface [11], leading to an excited triplet HONO species; the HONO(a^3A'') then absorbs a second photon at 193 nm to produce OH(A). Additionally in Kenner et al. [8], using two separate excimer lasers at 193 nm, the OH(A → X) emission intensity was observed to be dependent on the delay time between pulses from the two lasers, suggesting the decay of an excited intermediate species. However, the production of HONO(a^3A'') is energetically unfavorable when pumping HNO_3 at 248 nm, as excitation to the S_3 surface is not possible based on the current understanding of the HNO_3 potential energy surface [1,19].

The observed NO(A → X) fluorescence lifetime is long (~25–100 μs) when compared to the predicted lifetime (~8 μs); calculated from the upper limit quenching rate coefficient at room temperature and 50 Torr N_2 quoted in Settersten et al. [13]. This suggests an intermediate production route, or forbidden transition, which is causing a phosphorescence type process to occur. Unfortunately, it was not possible to elucidate whether an excited intermediate was present, as in Kenner et al. [8], when pumping at 248 nm, as the present study was limited to the use of a single excimer laser.

The temporal behavior of the fluorescence was characterized as a function of $[HNO_3]$ and $[N_2]$ using the PMT/optical filter setup (310 ± 5 nm). The emission at 310 nm was shown to have a biexponential decay, as shown in Fig. 4. The initial fast component was attributed to the combined laser scatter/saturation effect of the PMT with the OH(A) emission – a similar signal is observed at this time when there is no HNO_3 present in the apparatus. Several steps were taken to reduce the background fluorescence/scatter, however it was not possible to remove it entirely, and so a dependence of the early emission intensity as a function of $[HNO_3]$ was not possible.

The longer lifetime emission could not be unequivocally identified as a result of the poor signal to noise when using the spectrograph/ICCD combination. However, on comparison with the 193 nm experiments

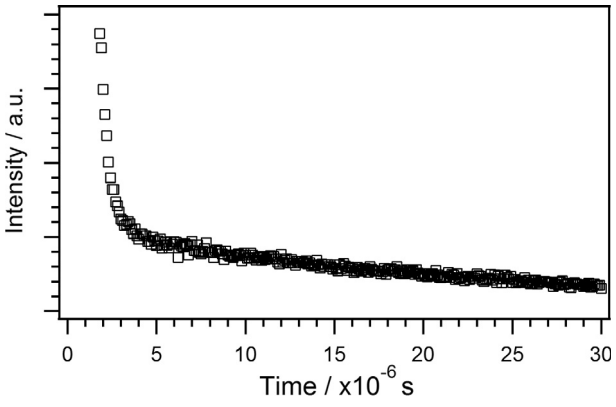

Fig. 4. Observed bi-exponential signal decay observed in the two-photon excitation of HNO_3 at 248 nm.

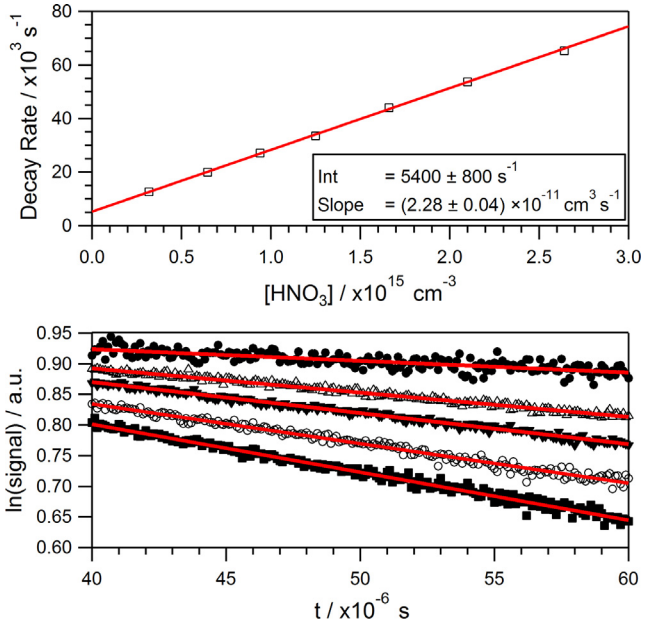

Fig. 5. Exponential decay fit (bottom panel) to determine the NO (A → X) fluorescence decay rate as a function of $[HNO_3]$ (top panel) from the two-photon excitation of HNO_3 at 248 nm. Data collected at 200 Torr N_2, 298 K, 100 ns bin integration, 2000 laser shots at 20 Hz excimer repetition frequency.

(Section 3.2.2), where the S/N ratio is significantly improved, it is assumed that the signal arises from multiple higher energy ro-vibrational transitions in the NO(A → X) band.

The longer emission lifetime was observed to decrease in proportion to $[HNO_3]$ (Fig. 5). Whilst the emission decay rate as a function of $[HNO_3]$ did not change significantly as the total N_2 pressure in the system was adjusted (50–750 Torr), the intercept was found to decrease with increasing pressure (8475–2944 s^{-1}, see Figure S3). This change in decay rate as a function of $[HNO_3]$ was used in our previous publication to characterize the $[HNO_3]$ for the OH + HNO_3 reaction using the LIF operating mode of the apparatus [18]. The LOD for this two photon method was determined as ~1.25×10^{14} cm^{-3} across all pressures (50–750 Torr), calculated from the minimum detectable decay greater than the intercept value based on the uncertainty in the decay rate vs $[HNO_3]$ plot (Fig. 5). The LOD is a significant improvement over the single photon detection method and the two photon method has enabled studies at ambient pressures.

Regular measurements of the decay rate as a function of $[HNO_3]$ were performed over a 6 month period; 8 times in total. Limited variability was observed in the decay rate dependence; e.g. at 200 Torr N_2, a standard deviation of 6.3% (± 2σ) was observed in the fitted linear regression coefficients. This error is equal to the reported error in the UV absorption cross section used to determine the $[HNO_3]$ [6], a commonly accepted reliable analytical approach.

3.2.2. 193 nm excitation

To elucidate the origin of the observed fluorescence signals in the two-photon pumping of HNO_3 at 248 nm, the emission spectrum was measured using two-photon pumping at 193 nm. The emission signal intensities were orders of magnitude greater in intensity than the 248 nm excitation case, allowing for a more extensive collection of data. Measurements using the PMT/Filter combination at ~308 nm were not possible due to PMT saturation. Altering the number of filters might have allowed the quantification of HNO_3 using this method, however this would have lowered the OH LIF sensitivity of the instrument required in the study of OH + HNO_3, making OH kinetic measurements increasingly difficult. Thus, these measurements at 193 nm serve only to help understand the nature of the HNO_3 PIF system.

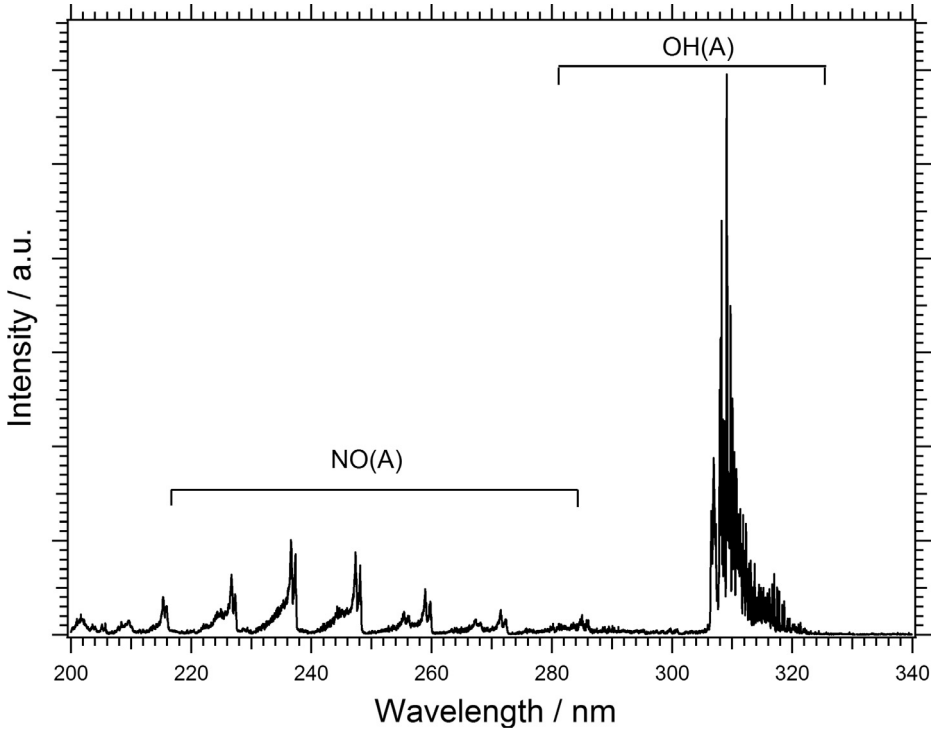

Fig. 6. Spectrum of the NO(A → X) and OH(A → X) emissions from the 2-photon photolysis of HNO_3 at 193 nm; 3000 laser shots.

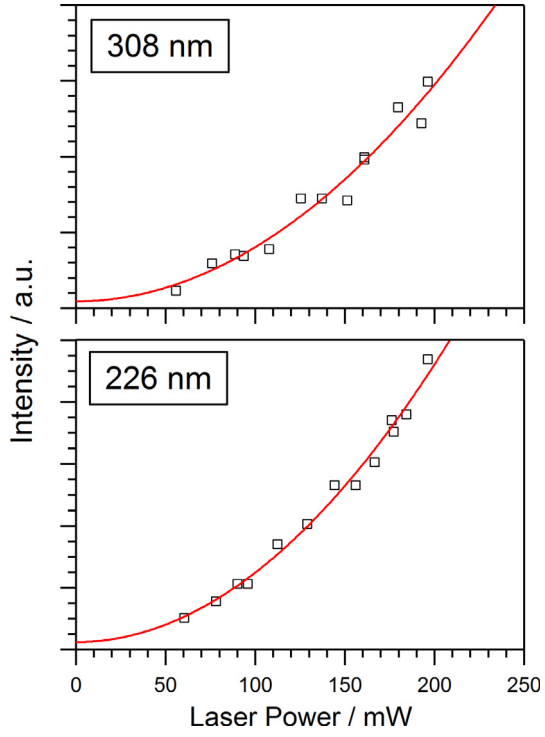

Fig. 7. Integrated signal intensity measured at 308 nm, OH($A \rightarrow X$, $v' = 0$, $v'' = 0$), and 226 nm, NO($A \rightarrow X$, $v' = 0$, $v'' = 0$), from the two photon photolysis of HNO_3 as a function of excimer laser power; $\lambda_{EX} = 193$ nm, 500 shots per point, $[HNO_3] = 1.5 \times 10^{15}$ cm^{-3}. Integrated signal was measured using the Spectrograph and ICCD. The excimer laser light was attenuated to achieve the lower laser powers required to observe a quadratic dependence of signal intensity with respect to laser power; data have been fit with a quadratic function, $y = y_0 + Ax^2$.

The emission spectrum was collected between 200 and 350 nm at 50 Torr N_2, $[HNO_3] \sim 1.5 \times 10^{15}$ cm^{-3}, averaged over 100 laser shots and with a focused excimer beam. The NO(A → X) and OH(A → X) emissions can be clearly identified; showing many of the same bands as the 248 nm photolysis case, see Fig. 6. Intensities measured at both 226 and 309 nm were observed to have a squared dependence with laser power at laser powers < 200 mW (Fig. 7). Above 200 mW, a saturation effect was observed and is discussed in more detail in the SOM. Emission intensities at 226 and 309 nm were observed to increase linearly with HNO_3 concentration (0.6–3.9 × 10^{15} cm^{-3}, Figure S4). Further experiments were conducted into the effects of changing bath gas pressure and collision partner (He and N_2) on the emission energy level population distributions, however the detailed analysis and discussion of these data sets are beyond the scope of this letter. The datasets are briefly described in the SOM.

The possible interference of NO_2 photolysis on the observed emissions was investigated. The ro-vibrational distribution of states from NO_2 photolysis matched very closely with HNO_3 case (Figure S5), and the intensity of NO(A) from NO_2 photolysis as a function of $[NO_2]$ (0.2–1.5 × 10^{15} cm^{-3}) was greater than for HNO_3. However, based on the total $[HNO_3]$ used, and the expected ~1% impurity of $[NO_2]$, the NO(A) observed in the HNO_3 photolysis case is unlikely from an NO_2 impurity or production of NO_2 followed by photolysis. Interestingly, OH (A → X) emission was observed in the NO_2 photolysis experiments, the intensity increasing proportionally to $[NO_2]$; the source of this emission is unknown (Figure S5). Additionally, OH(A → X) and NO(A → X) emissions were observed in the "background" measurement before HNO_3 or NO_2 were added to the system, indicating there was some HNO_3 diffusion from the cell surfaces into the bulk flow.

Examining the longer lifetime emissions around 308 nm (t_0 + 500 ns), higher energy ro-vibrational NO(A) bands were observed (Fig. 8). The observed NO(A → X) emissions can be easily assigned and we expect these to be the cause of the longer-lived emissions observed in the 248 nm photolysis case.

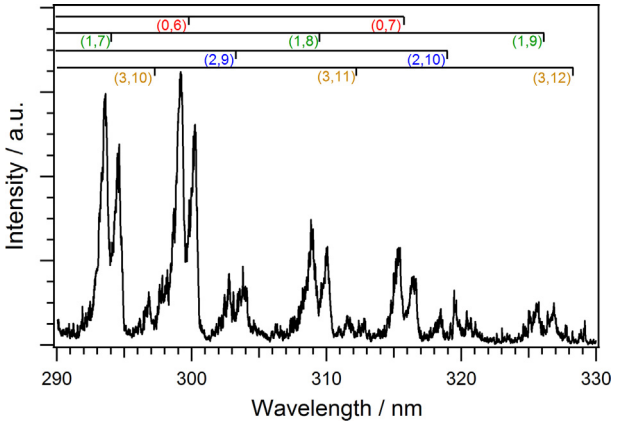

Fig. 8. Emissions assigned to higher energy ro-vibrational NO($A \rightarrow X$) bands from the two photon photolysis of HNO_3; λ_{EX} = 193 nm, 1000 laser shots, $[HNO_3] = 1.5 \times 10^{15}$ cm^{-3}, 350 Torr N_2.

4. Conclusions

The single and two photon initiated photodissociation of HNO_3 has been studied in bulk flows of N_2 and He bath gases using both single and two photons of 193 and 248 nm light. Extending the work by Kenner et al. [8] and, three major emissions from excited photodissociation products have been identified spectroscopically (NO(A), OH(A), $NO_2(^1B_2)$). The fluorescence has been studied over a range of pressures, $[HNO_3]$ and photolysis laser powers. The two photon photolysis work using 248 nm was extended to establish a unique method to quantify HNO_3 at the center of the LIF reaction cell. Utilizing the emission decay rate as a function of $[HNO_3]$, the two photon photolysis method was calibrated using an independent UV absorption measurement of HNO_3. The technique was found to be reproducible over a 6 month period, and expands the possible 2-photon detection methods already used in the literature for accurate quantification of HNO_3 in the laboratory [8,6]. This method was ultimately used in our publication into the kinetic determination of OH + HNO_3 rate coefficient [18].

Due to the complex nature of the emissions observed, the persistent background emission signals and the additional laser required for the OH + HNO_3 kinetic experiments, the two-photon photolysis of HNO_3 at 193 nm was not used to help quantify HNO_3, but rather to help identify longer lived emissions in the 308 nm region, which were used in the quantification procedure at 248 nm, establishing a unique method to quantify HNO_3 with good sensitivity and an ample limit of detection ($\sim 1.25 \times 10^{14}$ cm^{-3}).

Conflicts of interest

There are no conflicts to declare.

Acknowledgements

The experimental research was carried out by the Jet Propulsion Laboratory, California Institute of Technology, under contract with the National Aeronautics and Space Administration (NASA), and was supported by the Upper Atmosphere Research Program. Frank Winiberg's research was supported by an appointment to the NASA Postdoctoral Program, administered by Universities Space Research Association under contract with NASA.

Appendix A. Supplementary material

Supplementary data to this article can be found online at https://doi.org/10.1016/j.cpletx.2019.100029.

References

[1] Y.Y. Bai, G.A. Segal, Features of the electronic potential energy surfaces of nitric acid below 7 eV, J. Chem. Phys. 92 (1990) 7479–7483, https://doi.org/10.1063/1.458182.
[2] F. Biaume, Nitric acid vapour absorption cross-section spectrum and its photodissociation in the stratosphere, J. Photochem. 2 (1973) 139–149.
[3] S.S. Brown, R.K. Talukdar, A.R. Ravishankara, Reconsideration of the rate constant for the reaction of hydroxyl radicals with nitric acid, J. Phys. Chem. A 103 (1999) 3031–3037.
[4] P.S. Connell, C.J. Howard, Kinetics study of the reaction HO + HNO_3, Int. J. Chem. Kinet. 17 (1985) 17–31, https://doi.org/10.1002/kin.550170104.
[5] E.L. Derro, C. Murray, M.I. Lester, M.D. Marshall, Photodissociation dynamics of methyl nitrate at 193 nm: energy disposal in methoxy and nitrogen dioxide products, Phys. Chem. Chem. Phys. 9 (2007) 262–271, https://doi.org/10.1039/B614152H.
[6] K. Dulitz, D. Amedro, T.J. Dillon, A. Pozzer, J.N. Crowley, Temperature-(208–318 K) and pressure-(18–696 Torr) dependent rate coefficients for the reaction between OH and HNO_3, Atmos. Chem. Phys. 18 (2018) 2381–2394, https://doi.org/10.5194/acp-18-2381-2018.
[7] J.R. Huber, Photochemistry of molecules relevant to the atmosphere: photodissociation of nitric acid in the gas phase, ChemPhysChem 5 (2004) 1663–1669, https://doi.org/10.1002/cphc.200400071.
[8] R.D. Kenner, F. Rohrer, T. Papenbrock, F. Stuhl, Excitation mechanism for hydroxyl (A) in the argon fluoride excimer laser photolysis of nitric acid, J. Phys. Chem. 90 (1986) 1294–1299, https://doi.org/10.1021/j100398a018.
[9] A.K. Mollner, S. Valluvadasan, L. Feng, M.K. Sprague, M. Okumura, D.B. Milligan, W.J. Bloss, S.P. Sander, P.T. Martien, R.A. Harley, A.B. McCoy, W.P.L. Carter, Rate of gas phase association of hydroxyl radical and nitrogen dioxide, Science 330 (2010) 646–649, https://doi.org/10.1126/science.1193030.
[10] T.L. Myers, N.R. Forde, B. Hu, D.C. Kitchen, L.J. Butler, The influence of local electronic character and nonadiabaticity in the photodissociation of nitric acid at 193 nm, J. Chem. Phys. 81 (1997) 5361–5373.
[11] M. Nonella, H.U. Suter, J.R. Huber, An ab initio and dynamics study of the photodissociation of nitric acid HNO_3, Chem. Phys. Lett. 487 (2010) 28–31, https://doi.org/10.1016/j.cplett.2010.01.005.
[12] A. Schiffman, D.D. Nelson Jr., D.J. Nesbitt, Quantum yields for OH production from 193 and 248 nm photolysis of HNO_3 and H_2O_2, J. Chem. Phys. 98 (1993) 6935–6946.
[13] T.B. Settersten, B.D. Patterson, J.A. Gray, Temperature- and species-dependent quenching of NO AΣ+2(v′=0) probed by two-photon laser-induced fluorescence using a picosecond laser, J. Chem. Phys. 124 (2006) 234308, , https://doi.org/10.1063/1.2206783.
[14] A. Sinha, R.L. Vanderwal, F.F. Crim, The vibrationally mediated photodissociation dynamics of nitric acid, J. Chem. Phys. 91 (1989) 2929–2938, https://doi.org/10.1063/1.456963.
[15] R.A. Stachnik, L.T. Molina, M.J. Molina, Pressure and temperature dependences of the reaction of OH with nitric acid, J. Phys. Chem. 90 (1986) 2777–2780, https://doi.org/10.1021/j100403a044.
[16] A.A. Turnipseed, G.L. Vaghjiani, J.E. Thompson, A.R. Ravishankara, Photodissociation of HNO_3 at 193, 222, and 248 nm: Products and quantum yields, J. Chem. Phys. 96 (1992) 5887–5895.
[17] P.H. Wine, A.R. Ravishankara, N.M. Kreutter, R.C. Shah, J.M. Nicovich, R.L. Thompson, D.J. Wuebbles, Rate of reactions of OH with HNO_3, J. Geophys. Res. 86 (1981) 1105–1112.
[18] F.A.F. Winiberg, C.J. Percival, R. Shannon, M.A.H. Khan, D.E. Shallcross, Y. Liu, S. Sander, Reaction kinetics of OH + HNO_3 under conditions relevant to the upper troposphere/lower stratosphere, Phys. Chem. Chem. Phys 24652–24664 (2018), https://doi.org/10.1039/c8cp04193h.
[19] H. Xiao, S. Maeda, K. Morokuma, Theoretical insight into the wavelength-dependent photodissociation mechanism of nitric acid, Phys. Chem. Chem. Phys. 18 (2016) 24582–24590, https://doi.org/10.1039/C6CP04713K.